Mon. Not. R. Astron. Soc. **386,** 1966–1978 (2008) doi:10.1111/j.1365-2966.2008.12938.x

Effect of angular momentum distribution on gravitational loss-cone instability in stellar clusters around a massive black hole

E. V. Polyachenko,[1*] V. L. Polyachenko[1] and I. G. Shukhman[2*]

[1]*Institute of Astronomy, Russian Academy of Sciences, 48 Pyatnitskya St, Moscow 119017, Russia*
[2]*Institute of Solar-Terrestrial Physics, Russian Academy of Sciences, Siberian Branch, PO Box 291, Irkutsk 664033, Russia*

Accepted 2008 January 9. Received 2008 January 9; in original form 2007 September 27

ABSTRACT

We study the small perturbations in spherical and thin disc stellar clusters surrounding a massive black hole. Because of the black hole, stars with sufficiently low angular momentum escape from the system through the loss cone. We show that the stability properties of spherical clusters crucially depend on whether the distribution of stars is monotonic or non-monotonic in angular momentum. It turns out that only non-monotonic distributions can be unstable. At the same time, instability in disc clusters is possible for both types of distribution.

Key words: Galaxy: centre – galaxies: kinematics and dynamics.

1 INTRODUCTION

The study of the gravitational loss-cone instability, a far analogue of the plasma cone instability, began with the work of Polyachenko (1991), which dealt with a simple analytical model of a thin disc stellar cluster. Interest in the problem of the stability of stellar clusters was revived recently by detailed investigations of low-mass clusters around massive black holes by Tremaine (2005) and Polyachenko, Polyachenko & Shukhman (2007, hereafter Paper I). Both papers considered the stability of small amplitude perturbations of stellar clusters with disc-like and spherical geometry.

Using the criterion of Goodman (1988), Tremaine (2005) has shown that thin discs with symmetric distribution functions (DFs) over angular momentum and an empty loss cone are generally unstable. In contrast, by analysing perturbations with spherical numbers $l = 1$ and $l = 2$, he deduced that spherical clusters with a monotonically increasing DF of angular momentum should generally be stable.

Later, we demonstrated (see Paper I) that spherical systems with non-monotonic distributions may be unstable for sufficiently small-scale perturbations $l \geqslant 3$, while the harmonics $l = 1, 2$ are always stable. For the sake of convenience, we have used two assumptions. The first is that the Keplerian potential of the massive black hole dominates over a self-gravitating potential of the stellar cluster (which does not mean that we can neglect the latter). Then, the characteristic time of system evolution is of the order of the orbit precessing time, which is slow, compared to typical dynamical (free-fall) time. Because a star makes many revolutions in its almost unaltered orbit, we can regard it as being 'smeared out' along the orbit in accordance with passing time, and we can study the evolution of systems made of these extended objects.

The second assumption is a so-called 'spoke approximation', in which a system consists of near-radial orbits only. This approximation was earlier suggested by one of the authors (Polyachenko 1989, 1991). The spoke approximation reduces the problem to a study of simple analytical characteristic equations controlling small perturbations of stellar clusters.

There are two questions that naturally arise in this context. First, does the instability remain when abandoning the assumption of strong radial elongation of orbits? Secondly, does the instability occur in spheres with monotonically increasing distributions in angular momentum if we consider smaller-scale perturbations with $l \geqslant 3$? The aim of this paper is to provide answers to these questions.

To achieve this task, we use a semi-analytical approach based on the analysis of integral equations for slow modes elaborated recently in Polyachenko (2004, 2005) for thin discs, and in Paper I for spherical geometry. Following Paper I, we restrict ourselves to studying monoenergetic models with DFs in the form:

$$F(E, L) = A\delta(E - E_0) f(L). \qquad (1.1)$$

The models specified by function $f(L)$ are suitable for studying the effects of angular momentum distribution on gravitational loss-cone instability. However, the Dirac δ-function allows us to reduce the integral equations for slow modes to one-dimensional integral equations, and to advance substantially in analytical calculations.

Several arguments can be brought in favour of our simplified approach. First of all, the Lynden–Bell derivative (see Paper I, equation 4.7) of the DF with respect to angular momentum L, keeping $J = L + I_1$ constant (here I_1 is the radial action) in the limit where the slow mode approximation is applicable, can be replaced by a derivative, keeping energy E constant

$$\left(\frac{\partial F}{\partial L}\right)_{LB} = \Omega_{\rm pr}\left(\frac{\partial F}{\partial E}\right)_L + \left(\frac{\partial F}{\partial L}\right)_E \approx \left(\frac{\partial F}{\partial L}\right)_E,$$

because $\Omega_{\rm pr}$ is small. Thus, the derivative over energy is not included in the slow integral equation, and we can loosely say that

*E-mail: epolyach@inasan.ru; shukhman@iszf.irk.ru

dependence on energy is only parametric. Another argument is that the results of an independent study by Tremaine (2005), who used a non-monoenergetic DF, are in agreement with our conclusions.

Section 2 is devoted to spheres, and Section 3 to thin discs with symmetric DFs. The sections are organized alike. First, we derive integral equations for initial DFs in the form of equation (1.1). Then, analytical and numerical investigations of these equations follow. We demonstrate that in contrast to the case of a near-Keplerian sphere, the loss-cone instability in discs takes place even for the monotonic DF, $\mathrm{d}f/\mathrm{d}|L| > 0$, provided the precession is retrograde and the loss cone is empty: $f(0) = 0$. Section 2 is complemented by a stability analysis of models with circular orbits, which of course does not belong to the class of monoenergetic models of the type of equation (1.1).

Finally, in Section 4, we discuss the results and some perspectives of further studies.

2 SPHERICAL SYSTEMS

2.1 Integral equation for slow modes in monoenergetic models

The slow integral equation, which was derived in Paper I (see equation 4.8 there), is neatly suited to near-Keplerian systems. In contrast to Paper I, here we do not assume a strong elongation of orbits (i.e. we go beyond the spoke approximation).

Because the energies of all stars are identical, the unperturbed DF depends on one variable only. It is convenient to use a dimensionless angular momentum $\alpha = L/L_{\mathrm{circ}}(E_0)$, where L_{circ} is the angular momentum on circular orbits, $L_{\mathrm{circ}}(E_0) = GM_{\mathrm{c}}/(2|E_0|)^{1/2}$, M_{c} is the central point mass and G is the gravitational constant. The frequency of stellar radial oscillations $\Omega_1(E_0) = (2|E_0|)^{3/2}/(GM_{\mathrm{c}})$ and the radius of the system $R(E_0) = GM_{\mathrm{c}}/|E_0|$ are independent of the angular momentum. To shorten notations, we omit E_0.

The normalization constant A is taken so that the mass of the spherical system surrounding the central mass is equal to M_G (we assume that the ratio $\epsilon \equiv M_G/M_{\mathrm{c}}$ is small: $\epsilon \ll 1$):

$$M_G = \int F\,\mathrm{d}\Gamma = 2(2\pi)^3 \int \frac{\mathrm{d}E}{\Omega_1(E)} \int_0^{L_{\mathrm{circ}}} L\,\mathrm{d}L F(E, L).$$

If we define the normalization of the dimensionless DF over angular momentum f (see equation 1.1) as $\int_0^1 \mathrm{d}\alpha\alpha\, f(\alpha) = 1$, then the normalization factor A in equation (1.1) is

$$A = \frac{\Omega_1 M_G}{16\pi^3 L_{\mathrm{circ}}^2}. \tag{2.1}$$

This allows us to represent the kernel of the integral equation (equation 4.8 in Paper I) in the form

$$P_{s,s'}^{(l)}(E, L; E', L') = \frac{8\pi^2(2l+1)}{R} C_l \mathcal{K}_{s,s'}^{(l)}(\alpha, \alpha').$$

Here, l is the index of the spherical harmonic, $C_l = \int_0^\infty \mathrm{d}z z^{-1}[J_{(l+1)/2}(z) J_{l/2}(z)]^2$ and $J_\nu(z)$ is the Bessel function.[1] The functions $\mathcal{K}_{s,s'}^{(l)}$ satisfy the condition $\mathcal{K}_{s,s'}^{(l)}(0, 0) = 1$; their explicit form is given later. Then, substitution of the DF in the form of equation (1.1) leads to the following integral equation:

$$\phi_s(\alpha) = 2\Omega_1 \epsilon C_l \sum_{s'=s_{\min}}^{l} s'^2 D_l^{s'} \int_0^1 \frac{\Omega_{\mathrm{pr}}(\alpha')\alpha'\,\mathrm{d}f(\alpha')/\mathrm{d}\alpha'}{\omega^2 - s'^2\Omega_{\mathrm{pr}}^2(\alpha')} \times \mathcal{K}_{s,s'}^{(l)}(\alpha, \alpha')\phi_{s'}(\alpha')\mathrm{d}\alpha'. \tag{2.2}$$

Here, $\phi_s(\alpha)$ is the Fourier harmonics of the radial part of the perturbed potential (for more details, see Paper I), $\Omega_{\mathrm{pr}}(\alpha)$ is the orbital precession rate, $s_{\min} = 1$ for odd l and $s_{\min} = 2$ for even l. The coefficients D are calculated by

$$D_l^s = \begin{cases} \dfrac{1}{2^{2l}} \dfrac{(l+s)!(l-s)!}{\{[(1/2)(l-s)]!\,[(1/2)(l+s)]!\}^2}, & |l-s| \text{ even}, \\ 0 & |l-s| \text{ odd}. \end{cases} \tag{2.3}$$

Recall that equation (2.2) is written in a non-inertial reference frame centred on the mass M_{c}. Then, the additional indirect potential arising from the acceleration of the frame should be considered (see, for example, Tremaine 2005)

$$\Phi^i(\boldsymbol{r}, t) = G\boldsymbol{r} \int \boldsymbol{r}' \frac{\delta\rho(\boldsymbol{r}', t)}{r'^3}\mathrm{d}V', \qquad \delta\rho = \int \delta f\,\mathrm{d}\boldsymbol{v},$$

where δf is the perturbation to the background DF. Tremaine (2005) argued that for secular perturbations, this indirect potential must be omitted. Indeed, in studying secular evolution we should consider perturbations δf averaged over Keplerian orbits. In this case, the perturbed density is a superposition of contributions of individual orbits, averaged over their periods. A special feature of a Keplerian orbit is that the average force from this orbit acting to the material point located at the focus of the ellipse is equal to zero. Care must be taken however, as the perturbation is not well defined for orbits with low angular momenta. Below we consider systems with a ‘small amount’ of stars with low angular momenta only (see also the discussion in Section 2.2.1).

By changing the unknown function

$$\left[\omega^2 - s^2\Omega_{\mathrm{pr}}^2(\alpha)\right]\varphi_s(\alpha) = \phi_s(\alpha)$$

equation (2.2) can be reduced to the linear eigenvalue problem

$$\left[\omega^2 - s^2\Omega_{\mathrm{pr}}^2(\alpha)\right]\varphi_s(\alpha) = 2\Omega_1\epsilon C_l \sum_{s'=s_{\min}}^{l} s'^2 D_l^{s'} \times \int_0^1 \Omega_{\mathrm{pr}}(\alpha')\alpha' \frac{\mathrm{d}f(\alpha')}{\mathrm{d}\alpha'} \mathcal{K}_{s,s'}^{(l)}(\alpha, \alpha')\varphi_{s'}(\alpha')\,\mathrm{d}\alpha'. \tag{2.4}$$

For almost radial orbits, when $\alpha \ll 1$ or eccentricity $e \equiv \sqrt{1-\alpha^2} \approx 1$, the precession rate is

$$\Omega_{\mathrm{pr}}(\alpha) = -\frac{2\epsilon\Omega_1}{\pi^2}\alpha[1 + O(\alpha^2)]. \tag{2.5}$$

For orbits with smaller eccentricity, the numerical coefficient preceding the small parameter $\epsilon\Omega_1$ is greater than $2/\pi^2$. Because of the suggestion that the characteristic frequencies of the problem under consideration are of the order of typical precession velocities, $\omega \sim \Omega_{\mathrm{pr}} \sim \epsilon\Omega_1$, it is convenient to change to the dimensionless frequencies, measured in the natural ‘slow’ frequency:

$$\bar{\omega} = \frac{\omega}{\epsilon\Omega_1}, \qquad \nu(\alpha) = -\frac{\Omega_{\mathrm{pr}}(\alpha)}{\epsilon\Omega_1}. \tag{2.6}$$

For spherical systems, the precession is retrograde (see Tremaine 2005, or Paper I), so $\nu(\alpha) > 0$. Then the dimensionless integral

[1] For $l = 1$, the coefficient C_1 can be calculated analytically: $C_1 = 4/3\pi^2 \approx 0.135$. Numerical calculations show decreasing C_l with increasing mode number l: $C_2 = 0.063$, $C_3 = 0.0373$, $C_4 = 0.025$, $C_5 = 0.018$, and so on.

equation becomes

$$[\bar{\omega}^2 - s^2\nu^2(\alpha)]\varphi_s(\alpha) = -2C_l \sum_{s'=s_{\min}}^{l} s'^2 D_l^{s'} \times \int_0^1 \nu(\alpha')\alpha' \frac{\mathrm{d}f(\alpha')}{\mathrm{d}\alpha'} \mathcal{K}_{s,s'}^{(l)}(\alpha,\alpha')\varphi_{s'}(\alpha')\,\mathrm{d}\alpha'. \tag{2.7}$$

To obtain the eigenfrequency spectrum for a model, it is necessary to compute first the kernels $\mathcal{K}_{s,s'}^{(l)}(\alpha,\alpha')$ (universal for all models), and the precession rate profile $\nu(\alpha)$ for the given model. The integration over Keplerian orbits is most conveniently expressed using the variable τ, which is connected with the current radius r and the true anomaly ζ of a star[2] as follows:

$$r = \frac{1}{2}R(1 - e\cos\tau), \qquad \cos\zeta = \frac{\cos\tau - e}{1 - e\cos\tau}. \tag{2.8}$$

Then, after some transformations, the kernel $\mathcal{K}_{s,s'}^{(l)}$ can be reduced to the form

$$\mathcal{K}_{s,s'}^{(l)}(\alpha,\alpha') = \frac{2}{(2l+1)\pi^2 C_l}\int_0^{\pi} \mathrm{d}\tau\, r\cos(s\zeta) \times \int_0^{\pi} \mathrm{d}\tau' r'\cos(s'\zeta')\mathcal{F}_l(r,r'). \tag{2.9}$$

Here, r' and ζ' specify the position of a star on the orbit with eccentricity e' corresponding to the variable τ', and the following notation is used:

$$\mathcal{F}_l(r,r') = \frac{\min(r,r')^l}{\max(r,r')^{l+1}}.$$

The expression for the precession rate can be obtained by transformation of equation (4.2) of Tremaine (2005) (see also Paper I):

$$\nu(\alpha) = \frac{\alpha}{4\pi e}\int_0^{\pi} \frac{\mu(r)(\cos\tau - e)\mathrm{d}\tau}{r^2}, \tag{2.10}$$

and

$$\nu(1) = -\frac{1}{4}\pi\rho\left(\frac{1}{2}R\right).$$

Here, the density $\rho(r)$ is defined by equation (2.12).

For monoenergetic models, the minimal and maximal radii are $R_{\min} = (1/2)\,R\,(1 - e_{\max})$, $R_{\max} = (1/2)\,R\,(1 + e_{\max})$, where $e_{\max} = (1 - h^2)^{1/2}$ and h is the minimal dimensionless angular momentum corresponding to the boundary of the loss cone.

The function $\mu(r)$ is the ratio of the mass of a spherical system inside the sphere of radius r to the total mass M_G:

$$\mu(r) = \frac{\mathcal{M}_G(r)}{M_G}, \quad \mathcal{M}_G(r) = 4\pi\int_{R_{\min}}^{r} r'^2\rho(r')\,\mathrm{d}r'. \tag{2.11}$$

$M_G = \mathcal{M}_G(R_{\max})$, and the density is calculated by

$$\rho(r) = \frac{4\pi A}{r}\int_0^{L_{\max}(r)} \frac{f(L)L\,\mathrm{d}L}{\sqrt{L_{\max}^2 - L^2}} = \frac{M_G}{\pi^2 r R^2}\bar{\rho}(r),$$
$$\bar{\rho}(r) = \int_0^{\alpha_{\max}(r)} \frac{2\alpha\,\mathrm{d}\alpha\,f(\alpha)}{\sqrt{\alpha_{\max}^2 - \alpha^2}}, \tag{2.12}$$

where $\alpha_{\max} = \sqrt{4(r/R)(1 - r/R)}$. Hereafter, we assume $R = 1$.

[2] True anomaly is the angle between directions to the star and to the pericentre.

Using equations (2.8) and (2.10)–(2.12), we can transform the expression for the scaled precession rate $\nu(\alpha)$ to a more universal form:

$$\nu(\alpha) = \frac{\alpha}{2\pi^2 e^2}\int_0^1 \mathrm{d}\alpha'\alpha' f(\alpha')\mathcal{Q}(\alpha,\alpha'). \tag{2.13}$$

Here, the kernel $\mathcal{Q}(\alpha,\alpha')$ does not depend on a DF and equals

$$\mathcal{Q}(\alpha,\alpha') = 4\int_{p_{\min}}^{p_{\max}} \mathrm{d}r\sqrt{\frac{(r - r_{\min})(r_{\max} - r)}{(r - r'_{\min})(r'_{\max} - r)}}, \tag{2.14}$$

with $p_{\min} = \max(r_{\min}, r'_{\min})$, $p_{\max} = \min(r_{\max}, r'_{\max})$. Here, $r_{\min} = (1/2)\,(1 - e)$, $r_{\max} = (1/2)\,(1 + e)$, $r'_{\max} = (1/2)\,(1 - e')$, $r'_{\max} = (1/2)\,(1 + e')$ and $e = (1 - \alpha^2)^{1/2}$, $e' = (1 - \alpha'^2)^{1/2}$. For near-radial orbits $\mathcal{Q}(0, 0) = 4$, so we obtain the above-mentioned result (equation 2.5): $\nu \approx (2/\pi^2)\alpha$.

2.2 Analytical results

2.2.1 Exact solution with zero frequency for the lopsided mode (l = 1)

Tremaine (2005) has noted that for an arbitrary distribution $F(E, L)$ with empty loss cone, $F(E, L = 0) = 0$, a zero frequency lopsided mode $l = 1$ must exist. The mode corresponds to a non-trivial perturbation arising under the shift of the spherical system as a whole relative to the central mass. The perturbed potential in such a mode is

$$\delta\Phi(r,\theta) = -\xi\cos\theta\frac{\mathrm{d}\Phi_G}{\mathrm{d}r},$$

where ξ is the displacement. In terms of the function $\phi_{s=1}(\alpha)$, this perturbation has the form

$$\phi_1(\alpha) = \frac{e}{\alpha}\nu(\alpha), \tag{2.15}$$

or in terms of the function $\varphi_1(\alpha)$ from equation (2.7),

$$\varphi_1(\alpha) = \frac{e}{\alpha\nu(\alpha)}. \tag{2.16}$$

We can check that equation (2.15) and $\bar{\omega} = 0$ provided the condition

$$f(\alpha = 0) = 0$$

is a solution of equation (2.2) or (2.7) for $l = 1$, taking into account equations (2.13) and (2.14), written in the form

$$\mathcal{Q}(\alpha,\alpha') = -\frac{16}{\alpha'}\frac{\partial}{\partial\alpha'}\int_{p_{\min}}^{p_{\max}} \mathrm{d}r\sqrt{(r - r_{\min})(r_{\max} - r)} \times\sqrt{(r - r'_{\min})(r'_{\max} - r)},$$

and also the expression for the kernel $\mathcal{K}_{11}^{(1)}(\alpha,\alpha')$

$$\mathcal{K}_{11}^{(1)}(\alpha,\alpha') = \frac{6}{ee'}\int_{p_{\min}}^{p_{\max}} \mathrm{d}r\sqrt{(r - r_{\min})(r_{\max} - r)} \times\sqrt{(r - r'_{\min})(r'_{\max} - r)}.$$

The lopsided solution with zero frequency is specific for spherical systems. At first glance, it defies common sense to argue that the stationary mode in which the centre of mass of a spherical system does not coincide with the black hole is physical. Indeed, it seems that movement (oscillations) of the stellar cluster and the black hole relative to the common centre of mass must occur. However, it does not occur.

By all means, this is clear in the case of the empty loss cone of finite size, $h > 0$ (where h is the minimal value of the dimensionless angular momentum α, for which $f(\alpha) > 0$). Indeed, let us consider the spherically symmetric cluster. Because the loss cone is finite, there is a spherical empty cavity of finite radius in the centre of the sphere. According to Newton's first theorem (Binney & Tremaine 1987), in this cavity the black hole does not experience a net gravitational force from the cluster. Thus, if the black hole is initially deposited at some arbitrary point within the cavity, it would remain at this position (and hence acceleration of the stellar cluster as a result of non-coincidence of the centres of mass does not occur).

When $h = 0$, the situation is not so obvious, but the net force acting to the black hole from the shifted spherical system can also be zero. In order to assure this, we should write down the indirect potential, taking into account the expression for perturbed density in the zero lopsided mode $\delta\rho = -\xi\cos\theta\,\mathrm{d}\rho/\mathrm{d}r$:

$$\Phi^i(\boldsymbol{r}, t) = -2\pi\xi G r\cos\theta \int_0^R \mathrm{d}r' \frac{\mathrm{d}\rho(r')}{\mathrm{d}r'} \int_0^\pi \cos^2\theta' \sin\theta'\,\mathrm{d}\theta'$$
$$= \frac{4\pi}{3} G r\cos\theta\,\xi\rho(0),$$

Hence, the condition for omitting the indirect potential is $\rho(0) = 0$. In the following, we suppose this condition to be fulfilled. The condition is not equivalent to the condition $f(\alpha = 0) = 0$, imposed on the DF for the existence of such a solution of our governing integral equation. However, it is equivalent to the stronger condition: $f(\alpha = 0) = f'(\alpha = 0) = 0$. Indeed, it is easy to show that if $f(\alpha) \propto \alpha^s$ for small α, then $\rho(r) \propto r^{(s-1)/2}$ for small r. So, the condition $s > 1$ must be fulfilled.

In contrast, in disc systems, the analogous $m = 1$ zero mode does not exist, because there is no analogue of Newton's first theorem.

The very existence of zero modes is crucial for the stability analysis of spherical clusters with monotonic distributions. Indeed, the role of the destabilizing contribution of the right-hand side of equation (2.7) falls off with an increase of the number l. So, it is expected that the most 'dangerous' modes correspond to the lowest values of l. However, it turns out that the $l = 1$ mode is neutrally stable, and the next dangerous mode $l = 2$ is stable. Note, however, that such a reasoning is not valid for systems with non-monotonic distributions.

2.2.2 *Stable mode in systems with near-radial orbits*

By analysing equation (2.7), it is easy to find one more analytical solution with the frequency $\bar{\omega} = \mathcal{O}(1)$ at arbitrary values of l, for models with highly elongated orbits. First, we note that the frequency of this stable mode corresponds to the resonance on the tail of a narrow distribution, and so it decays exponentially slowly. In this way, the mode differs from the unstable modes of interest, which have a resonance in the region where the distribution is localized (i.e. at $\alpha \lesssim \alpha_T$). Thus, they have characteristic frequencies and growth rates of the order of $\mathcal{O}(\alpha_T)$.

After setting $\bar{\omega} \sim 1 \gg \alpha_T$ in equation (2.7), omitting the second summand on the left-hand side, turning to the spoke approximation, and taking into account the equality

$$\sum_{s=s_{\min}}^{l} s^2 D_l^s = \frac{1}{4} l(l+1),$$

we find

$$\bar{\omega}^2 = \frac{2C_l}{\pi^2} l(l+1). \tag{2.17}$$

It is essential that this high-frequency mode is independent of details of the DF. Note also that in systems with prograde precession, this mode describes the well-known radial orbit instability (instead of the neutral oscillations).

2.2.3 *Variational principle*

Using equation (2.7), we can prove the following two important statements.

(i) For spherical system models with monotonic distributions $f(\alpha)$, the eigenfrequency squared, $\bar{\omega}^2$, must be a real number. This means that either the instability is absent completely, or aperiodic instability with $\mathrm{Re}\,\bar{\omega} = 0$ occurs.

(ii) Rotating (or oscillating) unstable modes may appear only in models with non-monotonic distributions.

Let us write equation (2.7) in the form

$$\bar{\omega}^2 \varphi_s(\alpha) = s^2 \nu^2(\alpha)\varphi_s(\alpha) - 2C_l \sum_{s'=s_{\min}}^{l} s'^2 D_l^{s'}$$
$$\times \int_0^1 g(\alpha') \mathcal{K}_{s,s'}^{(l)}(\alpha, \alpha') \varphi_{s'}(\alpha')\,\mathrm{d}\alpha', \tag{2.18}$$

where $g(\alpha) = \nu(\alpha)\alpha\,\mathrm{d}f(\alpha)/\mathrm{d}\alpha$. We multiply both parts of equation (2.18) by $s^2 D_l^s \varphi_s^*(\alpha)$, sum the result over s (where asterisk denotes the complex conjugation), and integrate over α with the weight $g(\alpha)$. Then we obtain

$$\bar{\omega}^2 \int_0^1 g(\alpha)\,\mathrm{d}\alpha \sum_{s=s_{\min}}^{l} s^2 D_l^s |\varphi_s(\alpha)|^2 = \int_0^1 \nu^2(\alpha) g(\alpha)\mathrm{d}\alpha$$
$$\times \sum_{s=s_{\min}}^{l} s^4 D_l^s |\varphi_s(\alpha)|^2 - 2C_l \int_0^1 \mathrm{d}\alpha \int_0^1 \mathrm{d}\alpha' \sum_{s=s_{\min}}^{l} \sum_{s'=s_{\min}}^{l}$$
$$\times (ss')^2 D_l^s D_l^{s'} \mathcal{K}_{s,s'}^{(l)}(\alpha, \alpha') \left[g(\alpha)\varphi_s^*(\alpha)\right] [g(\alpha')\varphi_{s'}(\alpha')]. \tag{2.19}$$

The reality of the coefficients of $\bar{\omega}^2$ on the left-hand side of equation (2.19) and the first term on the right-hand side is evident. With the help of equation (2.9), we can show that the kernel in equation (2.19) has the following property of symmetry:

$$\mathcal{K}_{s,s'}^{(l)}(\alpha, \alpha') = \mathcal{K}_{s',s}^{(l)}(\alpha', \alpha). \tag{2.20}$$

So, it is easy to see that the second term on the right-hand side is also real. Consequently, taking the imaginary part of equation (2.19), we obtain

$$\mathrm{Im}(\bar{\omega}^2) \int_0^1 g(\alpha)\,\mathrm{d}\alpha \sum_{s=s_{\min}}^{l} s^2 D_l^s |\varphi_s(\alpha)|^2 \equiv 0. \tag{2.21}$$

From the last equality, the statements formulated above follow immediately. If the function $g(\alpha)$ (or, equivalently, $\mathrm{d}f(\alpha)/\mathrm{d}\alpha$) has a constant sign, then the integral should be non-zero, and so $\mathrm{Im}(\bar{\omega}^2) = 0$. In contrast, when $\mathrm{Im}(\bar{\omega}^2) \neq 0$, the integral must be equal to zero. Consequently, the function $g(\alpha)$ should change its sign, that is, DF $f(\alpha)$ is non-monotonic.

Let us explain the term 'variational principle' used in the title of this subsection. Consider a dynamic equation in the form $\mathrm{d}^2\xi/\mathrm{d}t^2 \equiv -\omega^2\xi = -\hat{K}\xi$. Provided that the 'elasticity operator' $\hat{K}$ is Hermitian, the dynamic equation may be obtained from the conditions $\delta(\omega^2)/\delta\xi = 0$ and $\delta(\omega^2)/\delta\xi^* = 0$. Here $\delta\xi$ and $\delta\xi^*$ are considered formally as independent variations while the functional

ω^2 is

$$\omega^2 = \frac{\int \xi^*(\hat{K}\xi) w(\alpha)\,\mathrm{d}\alpha}{\int |\xi|^2 w(\alpha)\,\mathrm{d}\alpha}$$

($w(\alpha)$ is a non-negative weight function). In such a case, it is used to speak about the variational (or energy) principle; for example, see a review by Kadomtsev (1966) on the MHD stability of plasma. However, it is easy to see that if $\int |\xi|^2 w(\alpha)\,\mathrm{d}\alpha \neq 0$ for any non-trivial ξ, then ω^2 is real. Thus, usually (as is the case in the MHD stability theory of plasma, where $\hat{K}$ is Hermitian and $w > 0$) the notions 'variational principle' and the reality of ω^2 are identical. However, in our case the condition $\int |\xi|^2 w(\alpha)\,\mathrm{d}\alpha \neq 0$ is not satisfied for any non-trivial ξ, unless the DF is monotonic. Assuming that this condition is fulfilled, following the tradition that originates from plasma physics we say that the variational principle takes place. Only, in this case the dynamical equation can be interpreted mechanically, in terms of elastic forces.

Evidently, equation (2.21) is a serious obstacle to obtaining unstable rotating modes, which might need to be avoided. For instance, if we slightly change the initial monotonically increasing DF in a narrow region near $\alpha = 1$, to disappear quickly but smoothly, then a modified system would be practically indistinguishable from the initial one. However, then the variational principle breaks down. Could the discontinuous disappearance of $f(\alpha)$ at $\alpha = 1$ be considered as the violation of monotony for the DF?

This question has been known to be important since a stability study of stellar systems with isotropic DFs, $F = F(E)$ (Antonov 1960, 1962). The variational principle there required a DF to be a decreasing function of energy E, $F'(E) < 0$, everywhere. Systems with $F'(E) > 0$ need to be examined separately, which has been done in some cases (see, for example, Antonov 1971; Kalnajs 1972; Polyachenko & Shukhman 1972, 1973; Fridman & Polyachenko 1984). An essential difference in the second type of DF is in jumps to zero at the phase space boundary $E = E_{\mathrm{bound}}$. In fact, in this case there is an interval degenerated into the single point $E = E_{\mathrm{bound}}$ where $F(E)$ is decreasing.

We checked numerically on the possibility of the instability development being connected with the maximum on the edge of the DF domain. For this purpose, we computed the number of models smoothed near $\alpha = 1$. The computations showed no sign of instability, in contrast to isotropic distributions, $F = F(E)$. The reason for the tolerance of our present models is in fact that the kernels $\mathcal{K}$ of integral operators in equation (2.18) vanish for the circular orbit $\alpha = 1$. Thus, details of the initial distribution near-circular orbits cannot affect much the solutions of the integral equation (2.18).

The roles of the different terms in equation (2.18) can be easily understood. When $\partial F/\partial L > 0$, the first term on the right-hand side of equation (2.18) favours stabilization, while the second term gives destabilization (taking into account that the operator involved in this construction is self-adjoint and positively defined). In principle, this destabilizing effect could lead to instability. However, this is not the case because the stabilizing contribution exceeds the destabilizing contribution in all cases considered by Tremaine (2005), and in the present paper (see the following sections).

2.3 Unstable models

Instability boundaries in terms of the angular momentum dispersion $\alpha_T < (\alpha_T)_\mathrm{c}$ found in Paper I for the monoenergetic DF with

$$f(\alpha) = \frac{N}{\alpha_T^2}\left(\frac{\alpha^2}{\alpha_T^2}\right)^n \exp - \left(\frac{\alpha^2}{\alpha_T^2}\right), \tag{2.22}$$

(where N is the normalization constant, α_T is the dimensionless angular momentum dispersion and n is a real number) have a qualitative character only. Formally, these boundaries lie outside the validity of the spoke approximation, as $(\alpha_T)_\mathrm{c} \sim 1$. Obtaining such critical dispersions means only that the spoke models, in which $\alpha_T \ll 1$ by definition, are certainly unstable. So the quantitative determination of these boundaries with the help of the exact integral equation is required. The power–exp model (2.22) is studied in Section 2.3.1.

In Section 2.3.2, we study the simplest Heaviside model, consisting of two steps (at $\alpha = h_1$ and $\alpha = h_2$; both in the spoke approximation framework and using the exact integral equation)

$$f(\alpha) = \frac{2}{h_2^2 - h_1^2}\left[H(\alpha - h_1) - H(\alpha - h_2)\right], \quad h_1 < h_2 < 1 \tag{2.23}$$

where $H(\alpha)$ denotes the Heaviside function. Finally, in Section 2.3.3 we consider the log–exp model with DF

$$f(\alpha) = \frac{N}{\alpha_T^2}\ln\left(\frac{\alpha^2}{h^2}\right)\exp - \left(\frac{\alpha^2}{\alpha_T^2}\right), \tag{2.24}$$

for $\alpha \geqslant h$, and $f(\alpha) = 0$ for $\alpha < h$ (i.e. with the empty loss cone; N is the normalization constant).

2.3.1 *Power–exp model*

Following Paper I, here we consider the stability of model (2.22) with $n = 2$ and $n = 3$ relative to the spherical harmonic $l = 3$. We note that at the limit $\alpha_T \ll 1$, both these models were unstable (the stability boundaries obtained using spoke approximation were $(\alpha_T)_\mathrm{c} = 0.193$ for $n = 2$ and $(\alpha_T)_\mathrm{c} = 0.283$ for $n = 3$).

For distribution (2.22), we find

$$N^{-1} = \frac{1}{2}\int_0^{1/\alpha_T^2} z^n \exp(-z)\mathrm{d}z, \qquad z \equiv \frac{\alpha^2}{\alpha_T^2}.$$

In particular, for $\alpha_T \ll 1$, the normalization constant is $N = 2/(n!)$. From equation (2.12), we obtain

$$\bar{\rho}(r) = N\int_0^{\alpha_{\max}^2(r)/\alpha_T^2} \frac{z^n \mathrm{e}^{-z}\mathrm{d}z}{\sqrt{\alpha_{\max}^2 - z\alpha_T^2}}.$$

Further calculations of the density (2.12) and precession rate (2.13) profiles should be evaluated numerically.

Solutions of the integral equation (2.7) for $n = 2$ and $n = 3$ show similar behaviour. At small values of α_T, each model has one unstable mode. When increasing the dimensionless angular momentum dispersion α_T, the growth rate of the instability decreases, and then vanishes at some critical value $(\alpha_T)_\mathrm{c}$: for the model $n = 2$, $(\alpha_T)_\mathrm{c}^{(2)} \simeq 0.301$; for the model $n = 3$, $(\alpha_T)_\mathrm{c}^{(3)} \simeq 0.311$ (see Fig. 1). We conclude that the spoke approximation in this case is qualitatively correct, but quantitatively poor. The instability becomes saturated at some critical value $(\alpha_T)_\mathrm{c}$, while the discrepancy between exact and approximate values of $(\alpha_T)_\mathrm{c}$ for both models are not small.

Apart from the unstable mode, the spectrum of each model has a discrete mode, the growth rate of which is equal to zero at small α_T, and becomes negative with increasing α_T. This is just the weakly decaying mode with the frequency $\bar{\omega}^2 \approx 2C_l l(l+1)/\pi^2$ (at $\alpha_T \ll 1$), as mentioned in Section 2.2.2. The dependence of the frequency on l for this mode was one of the tests for the numerical code of the integral equation solver. Another test was detecting the zero lopsided mode $l = 1$ mentioned in Section 2.2.1.

The third test was the evaluation of $\bar{\omega}(\alpha_T)$ dependence in the spoke approximation limit. Assuming that $\bar{\omega} = 2\lambda\alpha_T/\pi^2$, and using

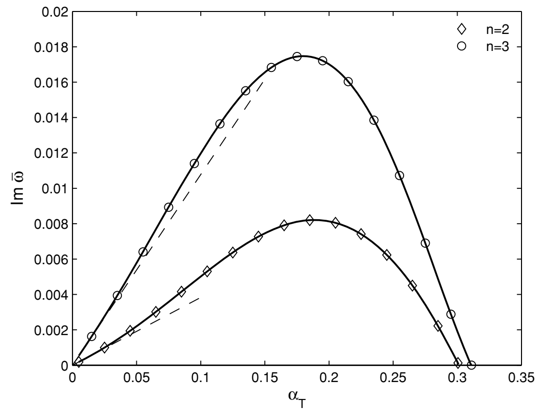

Figure 1. The dependence of the growth rate $\mathrm{Im}(\bar{\omega})$ versus the dimensionless angular momentum dispersion α_T of the mode $l = 3$ for models $n = 2$ (diamonds) and $n = 3$ (circles). Dashed lines show the asymptotic behaviour obtained using spoke approximation equation (2.25): $\mathrm{Im}(\bar{\omega}/\alpha_T) = (2/\pi^2)\mathrm{Im}\lambda$ with $\mathrm{Im}\lambda = 0.189$ and 0.532 for $n = 2$ and 3, respectively (the exact solution for $\alpha_T = 0.003$ gives 0.185 and 0.529).

$\mathcal{K}^{(l)}_{s,s'}(\alpha, \alpha') \approx 1$, $\phi_s(\alpha) \approx 1$, and $\nu(\alpha) \approx 2\alpha/\pi^2$ in equation (2.2), we can obtain the equation for the $l = 3$ mode

$$\int_0^\infty \mathrm{d}z(n - z)z^n \mathrm{e}^{-z} \left(\frac{1}{\lambda^2 - z} + \frac{15}{\lambda^2 - 9z} \right) = \mathcal{O}\left(\alpha_T^2\right). \qquad (2.25)$$

By setting the right-hand side to zero, we obtain an unstable mode for each n: $\lambda = 2.243 + 0.189i$ for $n = 2$ and $\lambda = 2.592 + 0.532i$ for $n = 3$. The same values obtained from a solution of the exact integral equation (2.7) for $\alpha_T = 0.003$ are $\lambda = 2.240 + 0.185i$ and $\lambda = 2.588 + 0.529i$, respectively.

2.3.2 *Heaviside model*

The simplest non-monotonic model that allows us to progress further with analytical methods is the model with a piecewise constant distribution over momentum (2.23). In other words, we assume the DF to be non-zero only within the interval $h_1 < \alpha < h_2$, where it is taken to be constant.

When studying the stability of discontinuous distributions such as equation (2.23), it is more convenient to start with the integral equation in the form of equation (2.2). Substituting equation (2.23) into equation (2.2), we obtain

$$\begin{aligned}\phi_s(\alpha) = \frac{4C_l\epsilon\Omega_1}{h_2^2 - h_1^2} \sum_{s'=s_{\min}}^{l} s'^2 D_l^{s'} \Bigg[&\frac{\Omega_{\mathrm{pr}}(h_1)h_1}{\omega^2 - s'^2\Omega^2_{\mathrm{pr}}(h_1)} \\ &\times \mathcal{K}^{(l)}_{s,s'}(\alpha, h_1)\phi_{s'}(h_1) - \frac{\Omega_{\mathrm{pr}}(h_2)h_2}{\omega^2 - s'^2\Omega^2_{\mathrm{pr}}(h_2)} \\ &\times \mathcal{K}^{(l)}_{s,s'}(\alpha, h_2)\phi_{s'}(h_2)\Bigg]. \end{aligned} \qquad (2.26)$$

Let us turn again to the natural slow scale of frequencies according to equation (2.6) and then substitute in equation (2.26) the particular values $\alpha = h_1$ and $\alpha = h_2$. For the sake of brevity, the following designations are used: $\nu_1 \equiv \nu(h_1)$ and $\nu_2 \equiv \nu(h_2)$. We have

$$\begin{aligned}\phi_s(h_1) = -\frac{4C_l}{h_2^2 - h_1^2} \sum_{s'=s_{\min}}^{l} s'^2 D_l^{s'} \Bigg[&\frac{\nu_1 h_1}{\bar{\omega}^2 - s'^2\nu_1^2} \mathcal{K}^{(l)}_{s,s'}(h_1, h_1) \\ &\times \phi_{s'}(h_1) - \frac{\nu_2 h_2}{\bar{\omega}^2 - s'^2\nu_2^2} \mathcal{K}^{(l)}_{s,s'}(h_1, h_2)\phi_{s'}(h_2)\Bigg], \end{aligned} \qquad (2.27)$$

$$\begin{aligned}\phi_s(h_2) = -\frac{4C_l}{h_2^2 - h_1^2} \sum_{s'=s_{\min}}^{l} s'^2 D_l^{s'} \Bigg[&\frac{\nu_1 h_1}{\bar{\omega}^2 - s'^2\nu_1^2} \mathcal{K}^{(l)}_{s,s'}(h_2, h_1) \\ &\times \phi_{s'}(h_1) - \frac{\nu_2 h_2}{\bar{\omega}^2 - s'^2\nu_2^2} \mathcal{K}^{(l)}_{s,s'}(h_2, h_2)\phi_{s'}(h_2)\Bigg]. \end{aligned} \qquad (2.28)$$

This set of equations relative to $\phi_s(h_1)$ and $\phi_s(h_2)$, ($s = 1, 2, \ldots, [(1/2)\,(l + 1)]$) can be reduced to the standard linear set. Introducing new unknown functions

$$X_s = \frac{\nu_1 h_1}{\bar{\omega}^2 - s^2\nu_1^2}\phi_s(h_1), \qquad Y_s = \frac{\nu_2 h_2}{\bar{\omega}^2 - s^2\nu_2^2}\phi_s(h_2),$$

we obtain

$$\begin{aligned}\left(\bar{\omega}^2 - s^2\nu_1^2\right) X_s = -4C_l \frac{\nu_1 h_1}{h_2^2 - h_1^2} &\sum_{s'=s_{\min}}^{l} s'^2 D_l^{s'} \\ &\times \left[\mathcal{K}^{(l)}_{s,s'}(h_1, h_1)X_{s'} - \mathcal{K}^{(l)}_{s,s'}(h_1, h_2)Y_{s'}\right], \end{aligned} \qquad (2.29)$$

$$\begin{aligned}\left(\bar{\omega}^2 - s^2\nu_2^2\right) Y_s = -4C_l \frac{\nu_2 h_2}{h_2^2 - h_1^2} &\sum_{s'=s_{\min}}^{l} s'^2 D_l^{s'} \\ &\times \left[\mathcal{K}^{(l)}_{s,s'}(h_2, h_1)X_{s'} - \mathcal{K}^{(l)}_{s,s'}(h_2, h_2)Y_{s'}\right]. \end{aligned} \qquad (2.30)$$

The precession rates in these equations can be expressed through the complete elliptical integrals $\boldsymbol{K}$ and $\boldsymbol{E}$:

$$\nu_1 = 2C_1 \frac{h_1}{e_1} \frac{1 - q^2 Q(q)}{1 - q^2}, \qquad \nu_2 = 2C_1 \frac{h_2}{e_1} \frac{Q(q) - q}{1 - q^2},$$

where $C_1 = 4/(3\pi^2)$, $q = e_2/e_1$, $e_1 = \left(1 - h_1^2\right)^{1/2}$, $e_2 = \left(1 - h_2^2\right)^{1/2}$, and the function $Q(q)$ is

$$Q(q) = \frac{1}{2q^2}[(1 + q^2)\boldsymbol{E}(q) - (1 - q^2)\boldsymbol{K}(q)].$$

In the limit $h_2 \to h_1$, the frequencies ν_1 and ν_2 are coincident, $\nu_1 = \nu_2 = (2/\pi^2)\,(h/e)$, where $h = h_1 = h_2$ and $e = e_1 = e_2$. Note that a determinant of the set of equations (2.29) and (2.30) has a rank $2[(1/2)\,(l + 1)]$. In particular, for the mode $l = 1$, the rank is equal to 2. Roots of the determinant are calculated numerically. The difference $h_2 - h_1$ has a meaning of dispersion (i.e. it is analogous to the parameter α_T in our models with smooth distributions).

A simple analytical task is to ascertain that $\bar{\omega}^2 = 0$ is the eigenvalue of the determinant for $l = 1$. We have for $\mathcal{K}^{(1)}_{11}(\alpha, \alpha')$

$$\mathcal{K}^{(1)}_{11}(\alpha, \alpha') = e_< Q(\kappa), \qquad (2.31)$$

where $\kappa = e_</e_>$, $e_< = \min(e, e')$, $e_> = \max(e, e')$, $e = (1 - \alpha^2)^{1/2}$ and $e' = (1 - \alpha'^2)^{1/2}$. In particular,

$$\mathcal{K}^{(1)}_{11}(h_1, h_1) = e_1, \qquad \mathcal{K}^{(1)}_{11}(h_2, h_2) = e_2, \qquad (2.32)$$

$$\mathcal{K}^{(1)}_{11}(h_1, h_2) = \mathcal{K}^{(1)}_{11}(h_2, h_1) = e_2 Q(q), \qquad q = e_2/e_1. \qquad (2.33)$$

Setting $\bar{\omega}^2 = 0$ in the determinant of the set of equations (2.29) and (2.30), and using the expressions for the elements of the kernel (2.32) and (2.33), we can show that it is equal to zero identically. This means the occurrence of a zero mode in the spectrum. Another root $\bar{\omega}^2$ for $l = 1$ is positive for any values of h_1 and h_2, which agrees with our previous conclusion (Paper I) that the instability is absent for the mode $l = 1$.

It is useful to derive in equations (2.29) and (2.30) in the spoke limit, when the distribution is localized in a region of small α. This

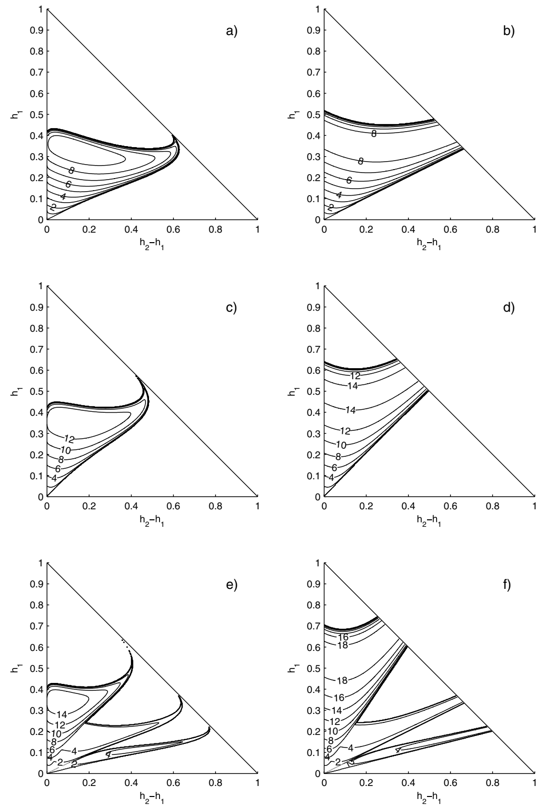

Figure 2. The stability boundaries and the isolines $10^2\mathrm{Im}(\bar{\omega})$ on the plane $(h_2 - h_1, h_1)$ for the Heaviside model. Left: exact calculations. Right: spoke approximation calculations. (a, b) For the mode $l = 3$; (c, d) for the mode $l = 4$; (e, f) for the mode $l = 5$. The spoke approximation is reliable in the lower-left corner of the domain. It is also seen that for $l = 3$, the growth rate sharply decreases when the ratio of the difference $h_2 - h_1$ (the analogue of the dispersion α_T for models with smooth DFs) to the size of the loss cone, h_1, becomes greater than 2.2.

means that we suggest $h_1 \ll 1, h_2 \ll 1, h_1 < h_2$, set in equation (2.26) $\phi_s(\alpha) = (-1)^s$, $\mathcal{K}^{(l)}_{s,s'} = (-1)^{s+s'}$. Finally, we obtain

$$1 = -\frac{4C_l}{h_2^2 - h_1^2} \sum_{s'=s_{\min}}^{l} s'^2 D_l^{s'} \left[\frac{\nu_1 h_1}{\bar{\omega}^2 - s'^2\nu_1^2} - \frac{\nu_2 h_2}{\bar{\omega}^2 - s'^2\nu_2^2} \right]. \quad (2.34)$$

For the precession frequencies ν_1 and ν_2, we have in this limit $\nu_1 = (2/\pi^2)h_1$, $\nu_2 = (2/\pi^2)h_2$. Introducing $\tilde{\omega} = (1/2)\pi^2\bar{\omega}$, let us write, for example, the characteristic equation for the mode $l = 3$. In this case, $D_3^1 = (3/16)$ and $D_3^3 = (5/16)$, hence

$$1 = -\frac{3\pi^2 C_3}{8} \frac{1}{h_2^2 - h_1^2} \times \left[\frac{h_1^2}{\tilde{\omega}^2 - h_1^2} + \frac{15h_1^2}{\tilde{\omega}^2 - 9h_1^2} - \frac{h_2^2}{\tilde{\omega}^2 - h_2^2} - \frac{15h_2^2}{\tilde{\omega}^2 - 9h_2^2} \right]. \quad (2.35)$$

Because of the denominator $h_2^2 - h_1^2 \ll 1$, the role of 'self-gravity' may be made sufficiently large in spite of the small parameter C_3. This may give the oscillating instability under certain conditions for h_1 and h_2. The limiting solutions serve as a test for the model with arbitrary h_1 and h_2.

The results for modes $l = 3$, $l = 4$ and $l = 5$ are presented in Figs 2(a)–(f). These show the boundaries of the instability domains on the plane $(h_2 - h_1, h_1)$. The left panels show the results of the computations from the exact set of equations (2.29) and (2.30); the right panels show the results from the spoke equation for this model (equation 2.34). It is seen that in the region $h_1 \ll 1$, $h_2 - h_1 \ll 1$, the results obtained from the spoke equation and those from the exact equations do coincide. The location of the growth rate maxima in Figs 2(a), 1(c) and (e), as well as the values of growth rates are practically the same.[3] We conclude that for the non-monotonic DF the instability is insensitive to the number l of the mode. This is a characteristic feature for the loss-cone instability. Recall that in models with monotonic distributions, the destabilizing term quickly decreases with increasing spherical number l of the mode.

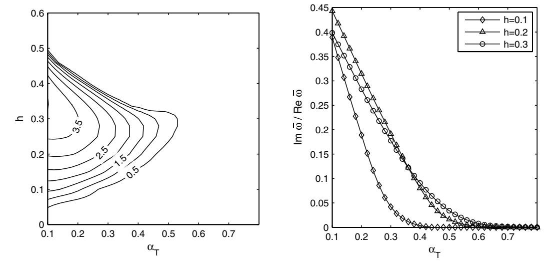

Figure 3. The mode $l = 3$ for the log–exp model. Left: isolines $10^2\mathrm{Im}\bar{\omega}$ on the plane (α_T, h). Right: the ratio of the growth rate $\mathrm{Im}(\bar{\omega})$ to the real part of the frequency $\mathrm{Re}\bar{\omega}$, for values $h = 0.1$, 0.2 and 0.3.

2.3.3 Log–exp model

In some numerical models (see, for example, Cohn & Kulsrud 1978; Berczik, Merritt & Spurzem 2005; Spurzem et. al. 2005) the initially isotropic distribution transforms under the action of a massive black hole into one monotonically increasing with angular momentum, $f(\alpha) \propto \ln(\alpha/h)$, where h defines the minimum angular momentum of a star that is not absorbed by the black hole. In this section, we consider the stability of DF (2.24). For this, we find

$$N^{-1} = \int_h^1 \frac{\mathrm{d}\alpha\alpha}{\alpha_T^2} \ln\left(\frac{\alpha^2}{h^2}\right) \exp - \left(\frac{\alpha^2}{\alpha_T^2}\right) = \frac{1}{2} \times \left[-\mathrm{Ei}\left(\frac{-h^2}{\alpha_T^2}\right) + \mathrm{Ei}\left(\frac{-1}{\alpha_T^2}\right) + \ln(h^2)\exp - \left(\frac{1}{\alpha_T^2}\right) \right],$$

where $\mathrm{Ei}(z)$ is the exponential integral. The density profile is obtained from equation (2.12):

$$\bar{\rho}(r) = \frac{N}{\alpha_T^2} \int_{h^2}^{\alpha^2_{\max}(r)} \frac{\mathrm{d}z}{\sqrt{\alpha^2_{\max}(r) - z}} \ln\left(\frac{z}{h^2}\right) \exp - \left(\frac{z}{\alpha_T^2}\right).$$

Much as in the power–exp model considered above, the calculations of the precession rate should be performed numerically.

The qualitative pattern of the spectrum for this model is similar to that of the power–exp model: when the dispersion is not too large, two discrete modes occur, one of which is unstable.

The left panel of Fig. 3 shows the isolines 10^2 $\mathrm{Im}\bar{\omega}$ on the plane of parameters (α, h) for the mode $l = 3$. A comparison of Figs 2 and 3 shows a qualitative coincidence of growth rate behaviour on the dispersion of the DF and the size of the loss cone in this and the Heaviside models. The right panel shows the ratio of the imaginary part to the real part of $\bar{\omega}$ versus the dimensionless angular momentum dispersion α_T for several values of loss-cone size parameter h.

[3] Two additional instability domains for $l = 5$ are explained by the more complicated structure of the characteristic equation for this mode, compared to the modes $l = 3$ and $l = 4$.

2.4 Stable models

The instability of spherical clusters around massive black holes was first studied by Tremaine (2005), who considered distributions of the form

$$f(I_1, I_2) \propto I_1^b \ln\left(\frac{I_2}{hI_1}\right) \tag{2.36}$$

in the domain $I_{\min} \leqslant I_1 \leqslant I_{\max}$, $I_2 > hI_1$ (and zero outside this domain). Here, I_r and $I_2 = L$ are the action variables, $I_1 = I_r + L$, and b and h are the real parameters. In the distribution, the loss cone is empty for dimensionless angular momentum $\alpha < h$. Tremaine studied the most large-scale perturbations with the spherical indices $l = 1$ and $l = 2$.

In this section we consider two monoenergetic models. The first is

$$f(\alpha) = N \ln\left(\frac{\alpha^2}{h^2}\right), \qquad h < \alpha < 1, \tag{2.37}$$

where $h < 1$ characterizes the size of the loss cone, and N is the normalization constant. The dependence of distributions (2.36) and (1.1) with $f(L)$ from equation (2.37) on the angular momentum is identical. This dependence is crucial for the stability or instability of each specific distribution. The stability of distribution (2.37) for arbitrary values of l is proved in Section 2.4.1.

Another distribution (Section 2.4.2) is the simplest monotonic Heaviside model in a form of the step-like DF,

$$f(\alpha) = \frac{2}{1-h^2} H(\alpha - h) H(1-\alpha). \tag{2.38}$$

The factor $H(1-\alpha)$ is added to reflect that the DF domain is bounded by circular orbits.

In Section 2.4.3, we prove the stability of spherical systems (in the field of a central massive body), all orbits of which are circular.

2.4.1 Log model

The distribution in the form of equation (2.37) allows us to calculate the density $\rho(r)$ explicitly. Using equation (2.12) we obtain

$$\bar{\rho}(r) = N \int_{h^2}^{\alpha^2_{\max}(r)} \frac{\mathrm{d}(\alpha^2)}{\sqrt{\alpha^2_{\max}(r) - \alpha^2}} \ln\left(\frac{\alpha^2}{h^2}\right), \tag{2.39}$$

where the normalization constant satisfies the relation

$$N^{-1} = \int_h^1 \mathrm{d}\alpha\alpha \ln\left(\frac{\alpha^2}{h^2}\right) = \frac{1}{2}\left[\ln\left(\frac{1}{h^2}\right) - (1-h^2)\right].$$

From the condition $h^2 \leqslant \alpha^2_{\max}(r) \equiv (4\,r/R)\,(1 - r/R)$, it follows that

$$R_{\min} = \frac{1}{2}R\left(1 - \sqrt{1-h^2}\right), \qquad R_{\max} = \frac{1}{2}R\left(1 + \sqrt{1-h^2}\right).$$

In the presence of the loss cone, $h > 0$, the radius of the system $R_{\max}$ is less than the apocentre radius for a radial orbit, R, as stars with low angular momentum, $\alpha < h$, are absorbed by the black hole. Integration (2.39) gives for the density

$$\bar{\rho}(r) = \frac{4}{R}\left[\sqrt{r(R-r)} \times \ln \frac{\sqrt{r(R-r)} + \sqrt{(r-R_{\min})(R_{\max}-r)}}{\sqrt{R_{\min}R_{\max}}} - \sqrt{(r-R_{\min})(R_{\max}-r)}\right].$$

As is seen, the density vanishes smoothly at the boundaries of the spherical layer $r = R_{\min}$ and $r = R_{\max}$. The expressions for the precession velocity are defined by equations (2.10) and (2.11).

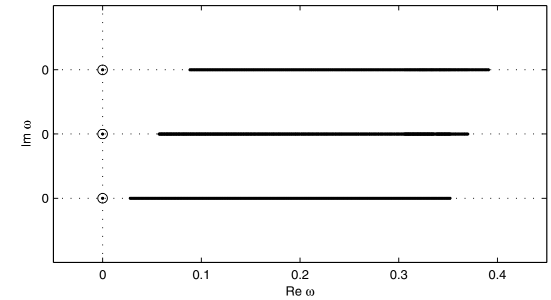

Figure 4. Spectrum for the log model with $h = 0.1$, 0.2 and 0.3 for $l = 1$. In all cases, the eigenfrequencies are neutral and consist of one zero mode (circled point) and the continuous part of the spectrum (points run into a line). To save room, the spectra are shown in a single plot, but vertically separated from one another (h increases from bottom to top).

Fig. 4 shows the frequency spectrum, $\bar{\omega}$, of the spherical harmonic $l = 1$ for the log model for different values of the parameter h. All calculations detect zero modes.

For other values of l (we have considered $l = 2$ and 3), the discrete modes are absent in the frequency spectra for all h. The spectra are continuous and lie at the region of real and positive values of $\bar{\omega}^2$. We conclude that the log models turn out to be stable.

2.4.2 Monotonic Heaviside model

Following the procedure described in Section 2.3.2 for the unstable Heaviside model, we can derive the following equation for the distribution function (2.38):

$$\phi_s(h) = -\frac{C_l}{C_1}\frac{2}{\sqrt{1-h^2}}\sum_{s'=s_{\min}}^{l} D_l^{s'} \frac{s'^2}{\lambda^2 - s'^2} \mathcal{K}^{(l)}_{s,s'}(h,h)\phi_{s'}(h), \tag{2.40}$$

where $\lambda = \bar{\omega}/\nu(h)$ and $\nu(h) = 8h/[3\,\pi^2\, e(h)]$. It is easy to see that for $l = 1$ there is a zero mode only, as $\mathcal{K}^{(1)}_{11}(h,h) = e(h) = (1-h^2)^{1/2}$. Introducing new variables $X_s = s\phi_s(h)\sqrt{D_l^s}/(\lambda^2 - s^2)$, we can reduce equation (2.40) to a standard linear set

$$\lambda^2 X_s = s^2 X_s - \sum_{s'=s'_{\min}}^{l} \hat{L}^{(l)}_{s,s'}(h) X'_s, \tag{2.41}$$

where the matrix

$$\hat{L}^{(l)}_{s,s'}(h) = 2\frac{C_l}{C_1}\frac{\mathcal{K}^{(l)}_{s,s'}(h,h)}{e(h)} ss' \sqrt{D_l^s D_l^{s'}}$$

is Hermitian. So, the eigenfrequencies λ^2 are real. Here again, we have a competition of opposite factors, expressed by the first and second terms on the right-hand side of equation (2.41). To conclude whether the instability occurs, we must find numerically zeros of the determinant $||(s^2 - \lambda^2)\delta_{s,s'} - \hat{L}^{(l)}_{s,s'}|| = 0$, as a function of λ^2 for $l \geqslant 2$. A rank of the determinant is equal to $[(1/2)\,(l+1)]$.

The results are represented in Figs 5 and 6, which show the dependence of $\lambda_j^2(h)$, $j = 1, 2, ..., [(1/2)\,(l+1)]$ as a function of the loss-cone size h. The instability is clearly absent. Each eigenvalue $\lambda_l^2(h)$ has only a weak dependence on h and approximately equals j^2. The least stable mode is $l = 3$ (see Fig. 6), but it is still far from instability.

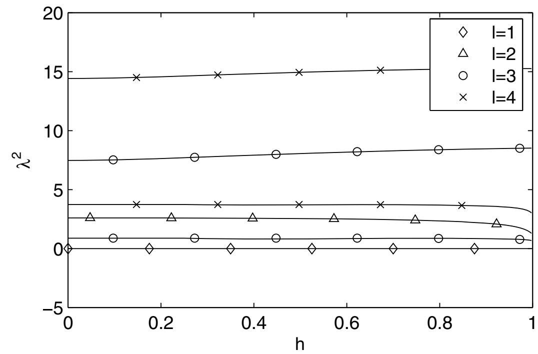

Figure 5. The dependence of the eigenfrequencies squared, $\lambda_j^2(h)$, for $l = 1, 2, 3$ and 4.

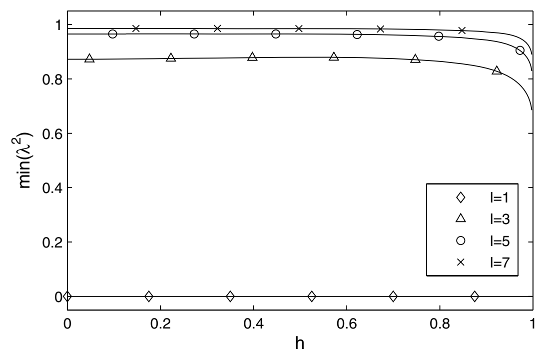

Figure 6. The dependence of the smallest (for given l) eigenfrequencies squared, $\lambda^2(h)$, for $l = 1, 3, 5$ and 7.

2.4.3 *Model with circular orbits*

Let us consider the simplest monotonic model, in which all orbits are circular. In this section, we do not assume a distribution to be monoenergetic, otherwise the density distribution would be degenerated to a thin spherical layer. Let us assume that the DF is $F(E, L) = A\delta\,[L - L_{\rm circ}(E)]$, where $A = $ const is the normalization factor and E changes in some range $\Delta\,E$. In terms of radial and transverse velocities v_r and $v_\perp = \sqrt{v_\theta^2 + v_\varphi^2}$, the DF is

$$F(v_r, v_\perp, r) = \frac{\rho_0(r)}{2\pi v_0(r)}\delta(v_r)\delta[v_\perp - v_0(r)], \quad v_0(r) = r\Omega(r),$$

where $\Omega(r)$ is the angular velocity of a star on the circular orbits. This velocity is determined by the balance of the centrifugal force and the sum of the gravitational forces from the central body and from the spherical cluster: $\Omega^2 = \Omega_0^2(r) + (1/r)\,{\rm d}\Phi_G(r)/{\rm d}r$, $\Omega_0^2(r) = GM_{\rm c}/r^3$. Here, we also suggest that $\Omega_0^2 \gg r^{-1}\,{\rm d}\Phi_G(r)/{\rm d}r$.

In this approximation, the orbits are near-Keplerian, and the following relations are valid:

$$\begin{aligned}
\omega_0^2 &\equiv 4\pi G\rho_0(r) = \Phi_G'' + \frac{2}{r}\Phi_G',\\
\Omega &= \Omega_0 + \frac{1}{2r\Omega_0}\Phi_G',\\
\kappa &= \Omega_0 + \frac{1}{2\Omega_0}\left(\Phi_G'' + \frac{3}{r}\Phi_G'\right).
\end{aligned} \qquad (2.42)$$

For the precession rate, we have (see also Tremaine 2001) $\Omega_{\rm pr} = \Omega - \kappa = -(1/2\Omega_0)[\Phi_G'' + (2/r)\Phi_G']$, or, taking into account equation (2.42), $\Omega_{\rm pr} = -(1/2)\,\omega_0^2/\Omega_0$. Because $\epsilon = M_G/M_{\rm c} \ll 1$, we have the following scalings, $\Omega_{\rm pr} \sim \epsilon\,\Omega_0$, $\omega_0^2 \sim \epsilon\,\Omega_0^2$, and for slow modes $\omega \sim \Omega_{\rm pr} \sim \epsilon\,\Omega_0$.

We start from the equation derived by Pal'chik et al. (1970), for models with circular orbits (this equation can also be found in the monograph by Fridman & Polyachenko 1984).[4] It has the form

$$\frac{\rm d}{{\rm d}r}r^2 A_l(r,\omega)\frac{{\rm d}\chi_l}{{\rm d}r} - B_l(r,\omega)\chi_l(r) = 0, \qquad (2.43)$$

where $\chi_l(r)$ is the radial part of the potential perturbation $\Phi(r) \propto \chi_l(r)\,Y_l^m(\theta, \varphi)\,\exp(-\,{\rm i}\omega t)$. Coefficients $A_l(r, \omega)$ and $B_l(r, \omega)$ are

$$A_l(r,\omega) = 1 + \omega_0^2 \sum_{s=-l}^{l} \frac{D_l^s}{[\omega - (s\Omega - \kappa)][\omega - (s\Omega + \kappa)]}, \qquad (2.44)$$

$$\begin{aligned}
B_l(r,\omega) &= l(l+1) + \sum_{s=-l}^{l} D_l^s\\
&\times \left[r^2 \frac{\rm d}{{\rm d}r}\left\{ \frac{\omega_0^2}{r}\frac{2s\Omega}{(\omega - s\Omega)[\omega - (s\Omega - \kappa)][\omega - (s\Omega + \kappa)]}\right\}\right.\\
&+ \omega_0^2 \left\{ \frac{4s\Omega(\omega - s\Omega) + s^2[(\omega - s\Omega)^2 + 4\Omega^2 - \kappa^2]}{(\omega - s\Omega)^2[\omega - (s\Omega - \kappa)][\omega - (s\Omega + \kappa)]}\right.\\
&+ \left.\left.\frac{(l+s+1)(l-s)}{(\omega - s\Omega)(\omega - s\Omega - 2\Omega)}\right\}\right].
\end{aligned} \qquad (2.45)$$

Now we need to distinguish between even and odd values of l, as l and s should be of the same parity (i.e. both even or both odd).

For even l, the dominating contributions are expected from $s = 0$ and $s = -2$. However, we can see that for even l, the contributions from $s = 0$ and $s = -2$ cancel out each other. Indeed, setting $\omega_0^2 = -2\Omega_0\Omega_{\rm pr}$ we have

$$A_l = 1$$

$$B_l = l(l+1) + D_l^0 l(l+1)\frac{\Omega_{\rm pr}}{\Omega} - D_l^2(l-1)(l+2)\frac{\Omega_{\rm pr}}{\Omega}.$$

After taking into account the relation

$$D_l^2 = D_l^0\left\{\frac{l(l+1)}{[(l-1)(l+2)]}\right\},$$

we obtain $A_l = 1$ and $B_l = l(l + 1)$. So, equation (2.43) is reduced to the trivial relation $\Delta\chi_l = 0$, which means the absence of slow density perturbations.

For odd l, the terms $s = \pm 1$ give the main contribution to the sum, while other terms ($|s| \neq 1$) are beyond the accuracy of the slow mode equation. Thus, we have

$$\begin{aligned}
A_l &= 1 + 2D_l^1\frac{\Omega_{\rm pr}^2}{\omega^2 - \Omega_{\rm pr}^2},\\
B_l &= l(l+1) - 4D_l^1 r^2 \frac{\rm d}{{\rm d}r}\left(\frac{1}{r}\frac{\Omega_{\rm pr}^2}{\omega^2 - \Omega_{\rm pr}^2}\right).
\end{aligned} \qquad (2.46)$$

To study this case, we transform the differential equation (2.43) with A_l and B_l from equation (2.46) to an integral equation. Equation (2.43) can be represented in the form of the Poisson equation

$$\Delta\chi_l(r) = 4\pi G\rho_l(r), \qquad (2.47)$$

[4] Note that in both the monograph and the original paper, the form of the equation does not allow the inclusion of the external gravitational field from a halo or a central body. We have slightly changed the equation to make this possible.

with the perturbed density

$$\rho_l(r) = -\frac{D_l^1}{4\pi G}\left\{\frac{1}{r^2}\frac{\mathrm{d}}{\mathrm{d}r}\left[r^2 S(\omega^2, r)\frac{\mathrm{d}\chi_l}{\mathrm{d}r}\right] + \frac{\mathrm{d}}{\mathrm{d}r}\left[\frac{2}{r}S(\omega^2, r)\right]\chi_l\right\}, \tag{2.48}$$

where $S(\omega^2, r) = 2\,\Omega_{\rm pr}^2/(\omega^2 - \Omega_{\rm pr}^2)$. The solution of equation (2.47) in the integral form is

$$\chi_l(r) = -\frac{4\pi G}{2l+1}\int r'^2\mathrm{d}r'\rho_l(r')\mathcal{F}_l(r, r') \tag{2.49}$$

where the kernel

$$\mathcal{F}_l(r, r') = \frac{(r')^l}{r^{l+1}}H(r - r') + \frac{r^l}{(r')^{l+1}}H(r' - r), \tag{2.50}$$

or, substituting equation (2.48) into equation (2.49), and integrating by parts,

$$\chi_l(r) = -\frac{D_l^1}{2l+1}\int \mathrm{d}r' S(\omega^2, r')\frac{\mathrm{d}}{\mathrm{d}r'}[r'^2\chi_l(r')] \times\left[\frac{\mathrm{d}\mathcal{F}_l(r, r')}{\mathrm{d}r'} + \frac{2}{r'}\mathcal{F}_l(r, r')\right]. \tag{2.51}$$

Applying the operator $\hat{\mathcal{P}}(r) = \mathrm{d}/\mathrm{d}r + 2/r$ to both parts of equation (2.51) and denoting $\Psi_l(r) = \hat{\mathcal{P}}(r)\chi_l(r) = \mathrm{d}\chi_l(r)/\mathrm{d}r + (2/r)\chi_l(r)$ we obtain an integral equation[5]

$$\Psi_l(r) = -\frac{D_l^1}{2l+1}\int r'^2\mathrm{d}r' S(\omega^2, r')\mathcal{R}_l(r, r')\Psi_l(r'), \tag{2.52}$$

with the new symmetrical kernel $\mathcal{R}_l(r, r') = (\mathrm{d}/\mathrm{d}r + 2/r)(\mathrm{d}/\mathrm{d}r' + 2/r')\mathcal{F}_l(r, r')$. Introducing the new function $Z_l = r\Omega_{\rm pr}/(\omega^2 - \Omega_{\rm pr}^2)\,\Psi_l$, we obtain the required integral equation

$$\left[\omega^2 - \Omega_{\rm pr}(r)^2\right]Z_l(r) = -\frac{2D_l^1}{2l+1}\int \mathrm{d}r'\Omega_{\rm pr}(r)\Omega_{\rm pr}(r') \times\mathcal{K}_l(r, r')Z_l(r'), \tag{2.53}$$

with the kernel $\mathcal{K}_l(r, r') = rr'\mathcal{R}_l(r, r')$.

Because the kernel defines a self-adjoint integral operator, all eigenfrequencies ω^2 should be real. To determine whether negative values of ω^2 are possible, let us write out the kernel $\mathcal{K}_l(r, r')$ explicitly:

$$\mathcal{K}_l(r, r') = -(l+2)(l-1)\mathcal{F}_l(r, r') + (2l+1)\delta(r - r'). \tag{2.54}$$

This contains two contributions: the first is negative, the second is positive. Substituting equation (2.54) into equation (2.53), we find

$$\omega^2 Z_l(r) = \Omega_{\rm pr}^2(r)\left(1 - 2D_l^1\right)Z_l(r) + 2D_l^1\frac{(l+2)(l-1)}{2l+1} \times\int \mathrm{d}r'\Omega_{\rm pr}(r)\Omega_{\rm pr}(r')\mathcal{F}_l(r, r')Z_l(r'). \tag{2.55}$$

For $l = 1$, we can see that $\omega^2 = 0$ satisfies this equation as $D_1^1 = (1/2)$. However, the most interesting fact is the stability of all higher modes, $l \geqslant 3$. Indeed, because $1 - 2D^l_1 > 0$ for $l \geqslant 3$, and the integral operator on the right-hand side is positively defined, we conclude that all eigenvalues, ω^2, are positive. Consequently, the instability is absent in the limit of circular orbits. The result is universal and does not depend on a particular choice of the model $\Omega_{\rm pr}$.

[5] The integral equation (2.52) can also be derived from the general 'slow' integral equation, by considering the circular orbit limit. However, this derivation is much more cumbersome than that given here.

3 THIN DISC SYSTEMS

3.1 Slow mode integral equation for monoenergetic disc models

In this section, we consider the monoenergetic distributions of the type of equation (1.1), assuming the function $f(\alpha)$ to be even, $f(\alpha) = f(-\alpha)$. The function $F(E, L)$ is normalized as follows:

$$M_G = \int F\mathrm{d}\Gamma = (2\pi)^2\int\frac{\mathrm{d}E}{\Omega_1(E)}\int_{-L_{\rm circ}(E)}^{L_{\rm circ}(E)}\mathrm{d}L\,F(E, L), \tag{3.1}$$

which gives the normalization constant

$$A = \frac{M_G}{\pi^2 R^2} \tag{3.2}$$

provided that $\int_{-1}^{1} f(\alpha)\mathrm{d}\alpha = 1$.

The integral equation for slow modes (Paper I) can be represented in the form

$$\phi(\alpha) = \frac{C_m}{\pi^3}\int_{-1}^{1}\frac{\mathrm{d}\alpha'\mathrm{d}f/\mathrm{d}\alpha'}{\bar{\omega} - \nu(\alpha')}\mathcal{K}_m(\alpha, \alpha')\phi(\alpha'), \tag{3.3}$$

or, using the evenness of $\phi(\alpha)$, which stems from the evenness of $f(\alpha)$, the oddness of $\Omega_{\rm pr}(\alpha)$, and the symmetry properties of the kernel, $\mathcal{K}_m(\alpha, \alpha') = \mathcal{K}_m(-\alpha, \alpha')$,

$$\phi(\alpha) = \frac{2C_m}{\pi^3}\int_0^1\frac{\nu(\alpha')}{\bar{\omega}^2 - \nu^2(\alpha')}\frac{\mathrm{d}f}{\mathrm{d}\alpha'}\mathcal{K}_m(\alpha, \alpha')\phi(\alpha')\mathrm{d}\alpha'. \tag{3.4}$$

Here, $\bar{\omega}$ and $\nu(\alpha)$ are the dimensionless pattern speed and the dimensionless precession rate:

$$\bar{\omega} = \frac{\Omega_p}{\epsilon\Omega_1}, \qquad \nu(\alpha) = \frac{\Omega_{\rm pr}(\alpha)}{\epsilon\Omega_1}. \tag{3.5}$$

Changing the unknown function, the integral equation (3.4) takes the form of the linear eigenvalue problem:

$$[\bar{\omega}^2 - \nu^2(\alpha)]\psi(\alpha) = \frac{2C_m}{\pi^3}\int_0^1\nu(\alpha')\frac{\mathrm{d}f}{\mathrm{d}\alpha'}\mathcal{K}_m(\alpha, \alpha')\psi(\alpha')\mathrm{d}\alpha'. \tag{3.6}$$

The kernel functions for thin discs $\mathcal{K}_m(\alpha, \alpha')$ can be transformed from the corresponding expression in Paper I to a suitable form, as follows:

$$\mathcal{K}_m(\alpha, \alpha') = \frac{1}{C_m}\int_0^{\pi}\mathrm{d}\tau r\cos m\zeta\int_0^{\pi}\mathrm{d}\tau' r'\cos m\zeta'\mathcal{F}_m(r, r'). \tag{3.7}$$

Here, the dependence of r and anomaly ζ on τ and e are the same as in the spherical case (equation 2.8), but the function $\mathcal{F}_m(x, y)$ is

$$\mathcal{F}_m(x, y) = \int_{-\pi}^{\pi}\frac{\cos m\theta\mathrm{d}\theta}{\sqrt{x^2 + y^2 - 2xy\cos\theta}}. \tag{3.8}$$

As before, the kernel $\mathcal{K}_m(\alpha, \alpha')$ is normalized to unity: $\mathcal{K}_m(0, 0) = 1$. This means that C_m is equal to

$$C_m = \int_0^1\mathrm{d}x\sqrt{\frac{x}{1-x}}\int_0^1\mathrm{d}y\sqrt{\frac{y}{1-y}}\mathcal{F}_m(x, y). \tag{3.9}$$

Equation (3.9) immediately follows from equation (3.7) if we remember that for radial orbits $\zeta = \pi$, $\cos m\zeta = (-1)^m$, $\mathrm{d}\tau = \mathrm{d}x[x(1-x)]^{-1/2}$. For the lowest azimuthal numbers, functions $\mathcal{F}_m(x, y)$ can be expressed through elliptical integrals of the first and second types $\boldsymbol{K}(q)$ and $\boldsymbol{E}(q)$:

$$\mathcal{F}_1(x, y) = \frac{4}{r_>}\frac{\boldsymbol{K}(q) - \boldsymbol{E}(q)}{q}, \tag{3.10}$$

$$\mathcal{F}_2(x, y) = \frac{4}{3r_>}\left[\left(\frac{2}{q^2}+1\right)\boldsymbol{K}(q) - 2\left(\frac{1}{q^2}+1\right)\boldsymbol{E}(q)\right], \quad (3.11)$$

where $r_> = \max(x, y)$, $r_< = \min(x, y)$ and $q = r_</r_>$. Using equations (3.10) and (3.11) we can obtain numerically $C_1 = 10.88$ and $C_2 = 7.45$.

For the surface density, we have

$$\sigma_0(r) = \frac{2}{r}\int \mathrm{d}E \int_{-L_{\max}(r)}^{L_{\max}(r)} \frac{F(E, L)\mathrm{d}L}{\sqrt{2E + (2GM_c/r) - (L^2/r^2)}}$$
$$= \frac{2M_G}{\pi^2 R^2}\Sigma_0(r), \quad (3.12)$$

where

$$\Sigma_0(r) = \int_{-\alpha_{\max}(r)}^{\alpha_{\max}(r)} \frac{f(\alpha)\mathrm{d}\alpha}{\sqrt{\alpha^2_{\max}(r) - \alpha^2}}, \quad (3.13)$$

and $\alpha^2_{\max}(r) = L^2_{\max}(r)/L^2_{\mathrm{circ}} = 4\,(r/R)\,(1 - r/R)$ as for spheres.

The relation between the precession rate and the potential $\Phi_G(r)$ is the same as in spherical systems (see Tremaine 2005 and Paper I)

$$\Omega_{\mathrm{pr}} = \frac{8}{\pi}\frac{1}{e\Omega_1 R^3}\int_0^{\pi} r^2 \frac{\mathrm{d}\Phi_G}{\mathrm{d}r}\cos\zeta\,\mathrm{d}\zeta. \quad (3.14)$$

However, the relation between the potential and the surface density is much more complicated [6] (see, for example, Tremaine 2001)

$$\Phi_G(r) = -\frac{4G}{r^{1/2}}\int (r')^{1/2}\sigma_0(r')\mathrm{d}r'[q^{1/2}\boldsymbol{K}(q)]. \quad (3.15)$$

Using equations (3.12)–(3.15), we obtain a suitable expression for the scaled precession rate $\nu(\alpha)$ (equation 3.5) in the integral form

$$\nu(\alpha) = \alpha\int_0^1 \mathrm{d}\alpha' f(\alpha')\mathcal{Q}(\alpha, \alpha'), \quad (3.16)$$

where $\mathcal{Q}(\alpha, \alpha')$ is a universal function (i.e. it does not depend on the form of the distribution):

$$\mathcal{Q}(\alpha, \alpha') = \frac{1}{\pi^3 e^2}\int_{r'_{\min}}^{r'_{\max}} \frac{r'\mathrm{d}r'}{\sqrt{(r' - r'_{\min})(r'_{\max} - r')}}$$
$$\times \int_{r_{\min}}^{r_{\max}} \mathrm{d}r\frac{2r - \alpha^2}{r\sqrt{(r - r_{\min})(r_{\max} - r)}}$$
$$\times\left[\frac{\boldsymbol{E}(\kappa)}{r' - r} - \frac{\boldsymbol{K}(\kappa)}{r' + r}\right]. \quad (3.17)$$

Here, $\kappa = 2\sqrt{rr'}/(r + r')$. The integral of the first term is understood in the principle value sense. Using the same trick as in Section 2, we can change to new integrating variables τ and τ', where $r = (1/2)\,(1 - e\cos\tau)$ and $r' = (1/2)\,(1 - e'\cos\tau')$. Then, for $\mathcal{Q}(\alpha, \alpha')$ we obtain

$$\mathcal{Q}(\alpha, \alpha') = \frac{1}{2\pi^3 e}\int_0^{\pi} \mathrm{d}\tau\frac{e - \cos\tau}{1 - e\cos\tau}\int_0^{\pi}\mathrm{d}\tau'(1 - e'\cos\tau')$$
$$\times\left[\frac{\boldsymbol{E}(\kappa)}{r' - r} - \frac{\boldsymbol{K}(\kappa)}{r' + r}\right]. \quad (3.18)$$

[6] For this reason, the precession in the near-Keplerian disc is not always retrograde.

3.2 Variational principle and sufficient condition for instability of the $m = 1$ mode

As seen from Section 2, for spherical systems with a monotonic DF, the variational principle takes place. Besides, for $l = 1$ and the empty loss cone, a zero frequency solution exists, which stands for a sphere displacement from the massive centre; all other eigenmodes are stable. A thin disc is completely different. The displacement is no longer an eigenmode. Moreover, models with analogous distributions turn out to be unstable. Let us prove the instability of the lopsided $m = 1$ mode provided that

$$g(\alpha) = \nu(\alpha)\mathrm{d}f/\mathrm{d}\alpha < 0. \quad (3.19)$$

Note that spherical models with an analogous condition are stable.

Discs with even DFs satisfying condition (3.19) obey the variational principle, which means the eigenfrequencies squared are real. So we can formulate a sufficient condition of instability for $m = 1$ azimuthal perturbations as follows. If the loss cone is empty [$f(0) = 0$], the DF is monotonically increasing $\mathrm{d}f/\mathrm{d}|\alpha| > 0$, and the precession is retrograde for all values of angular momentum ($\nu(\alpha)/\alpha < 0$), then $m = 1$ perturbations are unstable.

To prove the statement, we use integral equation (3.4), in which $\bar\omega = \mathrm{i}\Gamma$ with $\Gamma > 0$ is assumed:

$$\mathcal{M}(\Gamma)\phi(a) = 0. \quad (3.20)$$

Here, operator $\mathcal{M}(\Gamma)$ is

$$\mathcal{M}(\Gamma)\phi(a) \equiv \phi(a) + \frac{2C_m}{\pi^3}\int_0^1 \frac{g(\alpha')}{\Gamma^2 + \nu^2(\alpha')}$$
$$\times\mathcal{K}_m(\alpha, \alpha')\phi(\alpha')\mathrm{d}\alpha'. \quad (3.21)$$

Now we consider another eigenvalue problem

$$\mathcal{M}(\Gamma)\phi(a) = \lambda(\Gamma)\phi(a). \quad (3.22)$$

Eigenvalues Γ of problem (3.20) correspond to eigenvalues $\lambda(\Gamma) = 0$ of problem (3.22). Let us define an inner product as $\langle X, Y\rangle = \int_0^1 \mathrm{d}\alpha X^*(\alpha)W(\Gamma, \alpha)Y(\alpha)$, where the weight function $W(\Gamma, \alpha) = -g(\alpha)/[\Gamma^2 + \nu^2(\alpha)] > 0$. Operator $\mathcal{M}$ has the following properties.

(i) M is Hermitian, that is, $\langle\psi(a), M\phi(a)\rangle = \langle M\psi(a), \phi(a)\rangle = \langle\phi(a), M\psi(a)\rangle^*$.

(ii) M is continuous, when $\Gamma \geqslant 0$. It might be thought that the first term $\phi(a)$ on the right-hand side of equation (3.21) breaks down the continuity, which in turn means that the system of proper functions is incomplete. However, this is not the case, as $\phi(a)$ can be absorbed by introducing a new eigenvalue $\Lambda(\Gamma) = \lambda(\Gamma) - 1$ in equation (3.22). Because $f(\alpha)$ is even, for a smooth DF we have $f(0) = f'(0) = 0, f''(0) > 0$. This condition guarantees the weight function $W(\alpha)$ to be finite even for $\Gamma = 0$, despite $\nu = O(\alpha)$ at $\alpha \to 0$.

(iii) M is positive definite at sufficiently large Γ. This is evident, as $W(\alpha) > 0$, and the second term in equation (3.21) becomes small at large Γ.

From the first two properties, it follows that for fixed $\Gamma \geqslant 0$ eigenvalues $\lambda_n(\Gamma)$, $n = 1, 2, 3, \ldots$ of $\mathcal{M}(\Gamma)$ are real, and the system of proper functions is complete. The third property means that at large Γ all eigenvalues $\lambda_n(\Gamma)$ are positive.

If we find a test function $\phi_t(\Gamma_0, \alpha)$, for which the scalar product $\langle\phi_t(\Gamma_0, \alpha), \mathcal{M}(\Gamma_0)\phi_t(\Gamma_0, \alpha)\rangle$ is negative, this means that $\mathcal{M}(\Gamma_0)$ is not positive definite for given Γ_0. So, at least one eigenvalue must be negative: $\lambda_{\min}(\Gamma_0) < 0$. This minimal eigenvalue $\lambda_{\min}(\Gamma)$ increases with Γ and becomes positive, as all other $\lambda_n(\Gamma)$. We conclude that there must be a value of Γ, $\Gamma_0 < \Gamma < \infty$, for which $\lambda_{\min}(\Gamma) = 0$. This value is an eigenvalue for equation (3.21), which means the existence of the eigenmode describing aperiodic instability with growth rate Γ.

For the test function $\phi_t(\Gamma_0, \alpha)$, we can take a displacement of the disc from the centre, which is similar to the sphere displacement (2.15) and corresponds to the lopsided perturbation $m = 1$: $\phi_t(\Gamma_0, \alpha) = (e/\alpha)\,\nu(\alpha)$ and $\Gamma_0 = 0$. We can show that

$$\langle \phi_t(\Gamma_0, \alpha), \mathcal{M}(\Gamma_0)\phi_t(\Gamma_0, \alpha)\rangle < 0. \tag{3.23}$$

Let the left-hand side be $-P$, or explicitly

$$P = \int_0^1 \mathrm{d}\alpha \frac{\mathrm{d}f(\alpha)}{\mathrm{d}\alpha}\left[\frac{e(\alpha)}{\alpha}\right]^2 \nu(\alpha) + \frac{2C_1}{\pi^3}\int_0^1 \mathrm{d}\alpha \frac{e(\alpha)}{\alpha} \times \frac{\mathrm{d}f(\alpha)}{\mathrm{d}\alpha}\int_0^1 \mathrm{d}\alpha' \frac{e(\alpha')}{\alpha'}\frac{\mathrm{d}f(\alpha')}{\mathrm{d}\alpha'}\mathcal{K}_1(\alpha, \alpha').$$

After some lengthy manipulations using equations (3.7), (3.10), (3.18) and condition $f(0) = 0$, we can show that P is positive, so inequality (3.23) is fulfilled.

Tremaine (2005) has also obtained a sufficient condition for a lopsided mode in the symmetrical disc using the criterion of Goodman (1988). His condition, however, differs from ours. Namely, if the loss cone is empty, $F(E, L = 0) = 0$, and $\mathrm{d}\Phi_G(r)/\mathrm{d}r > 0$ throughout the radial range containing most of the disc mass, then the disc is unstable with respect to $m = 1$ perturbations. This formulation does not use the requirements that precession is retrograde and the DF is monotonically increasing, although a monotonic increase of $F(E, 0) = [\partial\, F(E, L)/\partial L]_{L=0} = 0$, $[\partial^2 F(E, L)/\partial L^2]_{L=0} > 0$ is implied, at least for small angular momentum. Thus, a comparison between spherical and disc cases can hardly be made, unless the conditions of stability are formulated in similar terms. To perform the comparison, we give our own criterion that follows directly from the integral equation.

It must be emphasized that the sufficient condition by Tremaine (2005) is different. Lack of the condition for the sign of precession possibly means that his criterion includes two types of instability simultaneously: the radial orbit instability arising in discs with prograde precession, and the loss cone instability that requires retrograde precession.

For discs composed of near-radial orbits, Tremaine's condition gives the result obtained in Paper I: a disc with symmetrical distribution $f(\alpha)$ obeying the conditions $f(0) = f'(0) = 0$, $f''(0) > 0$ is unstable if the precession is retrograde. In turn, the precession of near-radial orbits is retrograde if $\mathrm{d}\Phi_G(r)/\mathrm{d}r > 0$.

3.3 Numerical results

To support the mathematical rationale given above and to provide a basis for possible simulations, it is useful to obtain eigenfrequencies of unstable modes for particular models. Here we consider the power–exp model with symmetrical distribution

$$f(\alpha) = N\frac{\alpha^2}{\alpha_T^3}\exp\left(\frac{-\alpha^2}{\alpha_T^2}\right), \tag{3.24}$$

where the normalization constant is

$$N^{-1} = 2\int_0^{1/\alpha_T^2} x^2 \exp(-x^2)\mathrm{d}x.$$

For $\alpha_T \ll 1$, the constant $N = 2/\sqrt{\pi}$. Distributions become monotonic in the interval [0, 1] when $\alpha_T \geqslant 1$. Note that when $\alpha_T \gg 1$ the DF is simply $f(\alpha) = (3/2)\,\alpha^2$ in the interval $[-1, 1]$ and does not depend on α_T.

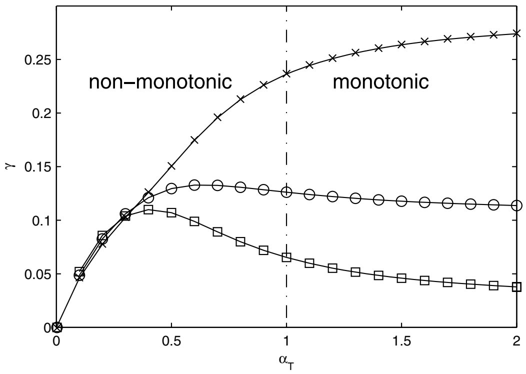

Figure 7. The dependence of γ (growth rate divided by azimuthal number m) versus dimensionless angular momentum dispersion α_T of the initial DF for azimuthal numbers $m = 1$ (crosses), $m = 2$ (circles) and $m = 3$ (squares).

Evaluation of integral equation (3.6) requires preliminary calculations of the kernel function $\mathcal{K}_m(\alpha, \alpha')$ using equation (3.7), and the scaled precession rate $\nu(\alpha)$ using equations (3.16) and (3.18). For brevity, we skip the details here, just noting that the calculation of function $Q(\alpha, \alpha')$ turns out to be a difficult numerical task. The calculations show that for model (3.18) the precession rate $\nu(\alpha)$ is retrograde for all α [i.e. $\nu(\alpha)/\alpha < 0$].

The results for values of azimuthal number $m = 1, 2, 3$ are collected in Fig. 7. Because the initial distribution is symmetric, the real parts of the eigenvalues $\bar{\omega}$ are equal to zero. Thus, in Fig. 7 we show the imaginary parts $\gamma = \mathrm{Im}\bar{\omega}$, which are the growth rates of the unstable modes divided by the azimuthal number m, versus the dimensionless angular momentum dispersion α_T. We can see that instability exists for all α_T and never becomes saturated. Moreover, it is easy to obtain the asymptotic values γ for different m at $\alpha_T \to \infty$: 0.289, 0.108 and 0.026 for $m = 1, 2, 3$, respectively. For small angular momentum, growth rates increase linearly with α_T, such that γ/α_T is equal to 0.454, 0.463 and 0.481 for $m = 1, 2, 3$, respectively.

4 DISCUSSION

We have studied the stability of spherically symmetric and thin disc stellar clusters around a massive black hole. We conclude that the stability properties of spherical clusters depend crucially on the monotonity of the initial DFs, while thin disc clusters are almost always unstable.

If the initial distribution of the spherical cluster is monotonic, the cluster is most likely to be stable. This conclusion was first made in Tremaine (2005), where the stability of the $l = 1$ mode was generally proved, and $l = 2$ was tested numerically. We confirm this conclusion by considering a number of monotonic distributions for modes with arbitrary l. Besides, we have checked distributions obtained from monotonic distributions by making them vanish quickly but smoothly at circular orbits. These models were also stable. However, we have not yet found a general proof of stability for any monotonic distributions.

Spherical clusters with non-monotonic DFs should be generally affected by the gravitational loss-cone instability. The instability was first found in Paper I using a simplification of systems with near-radial orbits. In Section 2 we have shown that this instability is a result of the non-monotony of distributions over angular momentum, and the orbits may not necessarily be near-radial.

In our opinion, both monotonic and non-monotonic distributions are important for possible applications to real stellar clusters around black holes. The DFs monotonically increasing from the loss-cone radius up to circular orbits are formed naturally as a result of two-body collisions of stars. This follows from numerical experiments (see, for example, Cohn & Kulsrud 1978), which predict the establishment of such distributions after a characteristic time for collisional relaxation. These distributions may be approximated by the formula $F \propto \ln(L/L_{\min})$.

Such a slowly increasing function is, in fact, predetermined by the boundary conditions imposed in the cited numerical study and some other investigations. Indeed, the vanishing condition at $L = L_{\min}$, and the matching condition to isotropic (Maxwellian) distribution, $F = F(E)$, at the boundary $E = E_{\rm bound} = 0$ of the phase space (E, L) (the boundary separates stars which is gravitationally coupled to the black hole from the others) is required. The latter condition means the asymptotic (when $E \to E_{\rm bound}$) independence of the function $F(E, L)$ from the momentum L. So monotonic, or logarithmic, dependence of the type of equation (2.37) is reasonable.

The non-monotonic distributions are also real. If the cluster is formed, for example, as a result of the collisionless collapse (several free-fall times), then it remains collisionless for a long time-scale of collisional relaxation (see, for example, Merritt & Wang 2005). In principle, the system can have an almost arbitrary DF in both the energy and the angular momentum. During the collapse, a typical non-monotonic distribution of stars over the angular momentum is formed, with empty loss cone and maximum at some value $L = L_*$.

In Paper I we argued that the stability properties of such a distribution are effectively analogous to one of the typical plasma distributions of 'beam-like' type. However, these can readily become unstable, as is well known in plasma physics (and also confirmed by the direct stability study of corresponding stellar systems in Paper I). It is possible (as is often so in plasma) that for the time of collisionless behaviour, the DF can undergo a dramatic change from its initial form. In particular, the collective flux of stars into the loss cone caused by the instability could, in principle, lead to the formation of a considerable part of the black hole. The checking of such possibilities is the most urgent task for future studies of unstable non-monotonic models.

Because spherically symmetric models with a monotonic DF are apparently stable, but analogous disc systems are unstable (see Tremaine 2005 and Section 3), we expect a critical flatness of ellipsoid models at which the instability begins. The study of such systems, as well as systems with more complex triaxial ellipsoids, can be performed using numerical simulations.

ACKNOWLEDGMENTS

We are grateful to V. A. Mazur for stimulating interest in our work. A careful review by the referee helped to improve the presentation. The work was supported in part by the Russian Science Support Foundation, RFBR grants nos 05-02-17874, 08-02-00928 and 07-02-00931, 'Leading Scientific Schools' grants nos 7629.2006.2 and 900.2008.2, the 'Young doctorate' grant no. 2010.2007.2 provided by the Ministry of Industry, Science, and Technology of Russian Federation, and the 'Extensive objects in the Universe' grant provided by the Russian Academy of Sciences. It was also supported by the Programmes of the Presidium of the Russian Academy of Sciences No 16 and OFN RAS No 16.

REFERENCES

Antonov V. A., 1960, Astron. Zh., 37, 918 (in Russian)
Antonov V. A., 1962, Vestnik Leningr. State Univ., 19, 96 (in Russian)
Antonov V. A., 1971, Uch. zap. Leningr. State Univ., 359, 64 (in Russian)
Berczik P., Merritt D., Spurzem R., 2005, ApJ, 633, 680
Binney J., Tremaine S., 1987, Galactic Dynamics. Princeton Univ. Press, Princeton, NJ
Cohn H., Kulsrud R. M., 1978, ApJ, 226, 1087
Fridman A. M., Polyachenko V. L., 1984, Physics of Gravitating Systems. Springer, New York
Goodman J., 1988, ApJ, 329, 612
Kadomtsev B. B., 1966, in Leontovich M. A., ed., Reviews of Plasma Physics: Hydromagnetic Stability of a Plasma, Vol. 2. Consultants Bureau, New York, p. 153
Kalnajs A. J., 1972, ApJ, 175, 63
Merritt D., Wang J., 2005, ApJ, 621, 101
Pal'chik M. Ya., Patashinsky A. Z., Pinus V. K., Epelbaum Ya. G., 1970, Preprint Inst. Nucl. Phys. Sb RAS, 99–100 (in Russian)
Polyachenko V. L., 1989, Sov. Astron. Lett., 15, 385
Polyachenko V. L., 1991, Sov. Astron. Lett., 17, 371
Polyachenko E. V., 2004, MNRAS, 348, 345
Polyachenko E. V., 2005, MNRAS, 357, 559
Polyachenko V. L., Shukhman I. G., 1972, Preprint SibIZMIR, No. 1-2-72, Irkutsk (in Russian)
Polyachenko E. V., Polyachenko V. L., Shukhman I. G., 2007, MNRAS, 379, 573 (Paper I)
Polyachenko V. L., Shukhman I. G., 1973, Astron. Zhurn., 50, 721 (English transl.: Sov. Astron., 17, 470)
Spurzem R., Giersz M., Takahashi K., Ernst A., 2005, MNRAS, 364, 948
Tremaine S., 2001, AJ, 121, 1776
Tremaine S., 2005, ApJ, 625, 143

This paper has been typeset from a TEX/LATEX file prepared by the author.